Title
ENHANCEMENT OF DIRECT PROCESSES IN HEAVY-ION REACTIONS AT HIGH ANGULAR MOMENTA

Author
Puhlhofer, P.

Publication Date
1972

Submitted to Nuclear Physics

ENHANCEMENT OF DIRECT PROCESSES IN HEAVY-ION REACTIONS AT HIGH ANGULAR MOMENTA

F. Pühlhofer and R. M. Diamond

January 1972

AEC Contract No. W-7405-eng-48

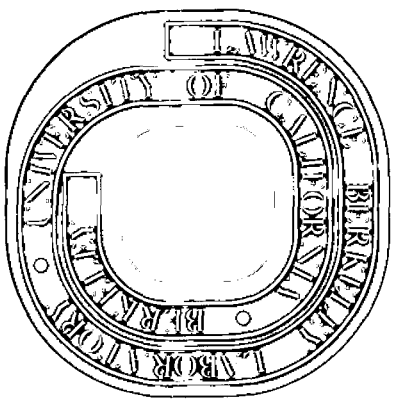

DISCLAIMER

ENHANCEMENT OF DIRECT PROCESSES IN HEAVY-ION REACTIONS AT HIGH ANGULAR MOMENTA†

F. Pühlhofer†† and R. M. Diamond

Lawrence Berkeley Laboratory
University of California
Berkeley, California 94720

January 1972

Abstract

Direct processes in reactions induced by ^{20}Ne on ^{27}Al were studied at incident energies from 4 to 10 MeV/nucleon using in-beam γ-ray spectroscopy. In addition to products from compound-nucleus reactions, several nuclei between A = 18 and 28 were identified, and it is shown that most of them are produced in direct reactions. The excitation functions for direct reactions reveal a threshold at about 100 MeV beam energy, above which the cross sections increase by an order of magnitude. A similar increase was also found in measurements with an ^{16}O beam of 6 to 10 MeV/nucleon on the same target. This behavior is explained as a consequence of the restriction of fusion processes due to the limitation on the angular momentum of the compound nucleus and a corresponding increase of the number of partial waves available for direct reactions.

---

†Work performed under the auspices of the U. S. Atomic Energy Commission.

††On leave of absence from the University of Marburg, Germany

1. Introduction

Heavy-ion reactions at energies far above the Coulomb barrier are characterized by large angular momenta between the interacting nuclei. This fact has an essential influence on the reaction mechanism. Using the liquid-drop model, Cohen, Plasil and Swiatecki[1]) have calculated that the angular momentum of a compound nucleus at which the fission barrier vanishes lies below the angular momenta involved, for example, in reactions induced by 200 MeV ^{20}Ne. Therefore, one expects the total compound-nucleus cross section to decrease at high bombarding energies. This has been confirmed experimentally by Kowalski, Jodogne and Miller[2]). They showed that the fusion cross section in the reactions between ^{16}O or ^{20}Ne and ^{27}Al drops significantly for beam energies above about 100 MeV. On the other hand, measurements by Wilkins and Igo[3]) show that the total reaction cross section in the system ^{16}O + ^{27}Al still increases slightly above 100 MeV.

From the fact that compound-nucleus formation cannot take place for high partial waves, one might expect a corresponding increase of the cross sections for direct reactions at higher energies. Whereas at lower energies only surface collisions contribute to direct reactions, a larger overlap between target and projectile will now be possible, and reactions like nucleon transfer should show increasing probability. However, the stronger interaction between the nuclei might also lead to more complicated reactions. The subject of the present work is a study of the direct processes in the system ^{20}Ne + ^{27}Al at beam energies between 4 and 10 MeV/nucleon. This system was chosen because it is expected that these effects become very pronounced for light nuclei at such beam energies[1]), and because measurements of the fusion cross section for this same reaction are published[2]). In addition, some measurements on the same target were done with

an ^{16}O beam.

The experiments were performed by measuring γ-rays from the residual nuclei, mainly in-beam. Information about the momentum transfer, and thus about the reaction mechanism, was obtained by means of the Doppler effect and by measuring the γ-intensities as a function of target thickness. The method applied here has the advantage that a large number of product nuclei can be observed in a relatively short bombardment time. Also, since the angular distributions of γ-rays are approximately isotropic, in particular for products from direct reactions, a single measurement at any angle is sufficient. This is in contrast to the detection of particles, which preferentially go to very small forward angles, thus making the observation with counter telescopes very difficult.

Several studies of the mechanism of heavy-ion reactions at beam energies up to 10 MeV/nucleon have been published. The measurements of the fusion cross section of Kowalski et al[2]) were extended to heavier target nuclei by Natowitz[4]). Sikkeland and Viola[5]) determined the relative amount of direct and compound-nucleus cross sections in heavy-ion reactions on ^{238}U and other heavy elements. Ladenbauer-Bellis et al[6]) measured excitation functions for several radioactive products in ^{12}C-, ^{14}N- and ^{16}O-induced reactions on ^{27}Al. Excitation functions for the same projectiles on ^{12}C and medium-mass targets have also been obtained at the Yale Hilac[7]). Anderson et al[8]) measured the reaction products emitted in the forward direction in the bombardment of ^{27}Al by 160 MeV ^{16}O and found cross sections of several hundred millibarns for non-compound processes. Reactions induced by ^{12}C and ^{16}O on targets ranging from ^{27}Al to heavy elements were investigated at the cyclotron in Dubna; Volkov and Wilczynski[9]) reported excitation functions for the (^{12}C,^{13}C) reaction and

Gridnev et al[10]) measured the energy spectra of the outgoing particles in several ^{16}O-induced reactions. Recently, Galin et al[11]) studied spectra and angular distributions of products of ^{14}N-induced reactions on Ag. However, most experiments do not give information about direct reactions and their excitation function in the energy range in which compound-nucleus reactions are expected to be appreciably hindered.

2. Experimental Method

The experiments were performed using ^{20}Ne and ^{16}O beams from the Hilac. Gamma-rays were detected by means of two Ge(Li) counters (1 cm^3 and 7 cm^3) placed approximately 90° to the beam on each side of the ^{27}Al target. Spectra were taken in-beam and in the 20 ms intervals between the 5 ms long beam bursts in order to distinguish the prompt transitions from isomeric ones and from γ-rays of daughter nuclei after β-decay.

The residual nuclei were identified only by the energy of their gamma transitions, but in the mass region in question the latter are generally known in detail. Absolute cross sections were determined from the known efficiency of the detectors assuming isotropy of the γ-radiation. This may cause errors of the order of 20 or 30% in the case of aligned compound nuclei, but for direct reactions the errors are expected to be smaller. The beam current was measured in a Faraday cup behind the target and corrected for the average charge state of the ions. The cross sections determined here are understood as cross sections for the production of a certain γ-ray; they are only lower limits for the formation of a final nucleus. Also it was not possible to distinguish whether a level is fed directly by a transfer reaction or via γ-deexcitation of higher excited states formed in the transfer.

Excitation functions were measured in large energy steps. The beam

energies were 85, 118, 149 and 206 MeV for ^{20}Ne and 96, 130 and 165 MeV for ^{16}O. The usual target thickness was 5.5 mg/cm^2, but information about the recoil of the residual nucleus was obtained by measuring the γ-intensities as a function of target thickness. In compound-nucleus reactions, the residual nucleus has a large recoil, which can be calculated assuming that it retains, on the average, the velocity of the compound nucleus even after evaporation of several particles. This leads to yield curves as shown in fig. 1. In particular, the γ-ray intensity of a slow transition ($\tau >> 1$ ns) after a compound-nucleus reaction is expected to be very small if the target thickness, d, is smaller than the range, R_{CN}, of the residual nucleus, because the recoiling nucleus leaves the target and gets out of the range of the detector before decaying. R_{CN} is calculated to be between 4.4 and 4.8 mg/cm^2 Al depending on the nucleus. Emission of a few α-particles will modify this yield curve only slightly. Direct reactions are characterized by small momentum transfers to the target nucleus, and the yield curves of the latter have always to be linear without a break, irrespective of the lifetime involved.

The recoil of a product nucleus can also be determined by means of the Doppler effect, which was observed particularly at the higher incident energies. Even if the detectors are placed at 90°, lines from recoiling compound nuclei have to show a broadening, because the Ge crystals cover a finite angular range (90 ± 25° for the 7 cm^3 detector). This fact enables one to get information about the reaction mechanism also in cases where the lifetime is much smaller than 1 ns. In direct reactions, the residual nuclei formed from the target nucleus will not have an appreciable recoil, whereas the ones formed from the projectile have essentially the velocity of the beam particles and will therefore give very broad lines.

3. Results

3.1 SPECTRA

The γ-spectra obtained with ^{20}Ne on ^{27}Al at 85 MeV (fig. 2) show many lines due to nuclei in the mass region A = 38 to 44; these are products of compound-nucleus reactions. At higher incident energies, the lines of ^{36}Cl and ^{32}P appear. At 206 MeV the spectra are characterized by γ-rays from nuclei with A = 18 to 28. Most of these nuclei are produced in direct processes. The arguments leading to this conclusion will be discussed later.

The energies of the γ-rays observed in the ^{20}Ne experiment and the corresponding nuclei are listed in table 1. A plot of these nuclei versus N and Z is shown in fig. 3. Although our experiments were very selective, in that a nucleus is required to have an intense γ-transition in the energy range from about 30 to 600 keV in order to be observed with high detection efficiency, it is seen that the residual nuclei are essentially confined to the valley of stability. In the case of compound-nucleus reactions this is due to the evaporation of α-particles, which is favored by the Q-value and the fact that α-particles may carry off more angular momentum from the high-spin compound nucleus. In the case of direct reactions the reasons are more complex, because of the presence of different types of reaction mechanisms.

An important feature of the spectra obtained with the ^{20}Ne beam at high energy is the occurrence of Doppler-broadened lines. A striking example is the 351 keV line of ^{21}Ne. It consists of two components: a sharp line, and a much more intense triangular-shaped component. The latter obviously comes from fast-moving ^{21}Ne nuclei formed by a pick-up of a neutron by the ^{20}Ne projectiles. The width (12% at the base of the line) agrees with that calculated from the known counter geometry and the velocity of the beam particles; the velocity of

the compound-nucleus would lead to less than half this width. The broad component of the ^{21}Ne line is strongly shifted in a spectrum taken with the counter at 50°, and it is, of course, absent in the spectra taken with the ^{16}O beam. The sharp component is due to ^{21}Ne formed either in a compound-nucleus reaction or more likely from the target in a direct reaction.

A very broad triangular-shaped line (roughly 10% width at the base) with E_γ = 1368 ± 5 keV was observed in a measurement with a coaxial counter at 149 MeV beam energy. It seems to be due to ^{24}Mg formed by an α-pick-up by the projectile. Its cross section is very large, approximately 150 ± 70 mb. There are also indications that a part of the 110 keV line originates from ^{19}F formed from ^{20}Ne in a proton-stripping process. The Doppler broadening is hard to observe in the spectra in this case because of the lower energy of the line and its proximity to the intense 106 keV line of ^{38}Ar. However, we see a shifted peak with the counter at 50°. The $1/2^-$ state at 110 keV in ^{19}F is a $p_{1/2}$-hole state which is likely to be formed in a stripping process.

The data show a clear asymmetry between neutron and proton transfer. Whereas ^{21}Ne, formed by a neutron pick-up by ^{20}Ne, is observed with large cross section, the analogous line of ^{21}Na (332 keV, τ = 14 ps) is not seen, which means that its cross section is at least a factor of 4 smaller. Both the proton and the neutron pick-up have essentially the same Q-value, and Coulomb energy effects[20]) are small. The only difference seems to be the fact that the proton is much less bound to ^{20}Ne than the neutron (2.5 and 6.8 MeV respectively). Unfortunately, we are not able to compare directly with the corresponding stripping processes, because the states in ^{19}F and ^{19}Ne, which are most likely to be populated ($5/2^+$ states at 197 and 238 keV respectively), are long-lived and cannot be observed when formed from the projectile.

3.2 RECOIL MEASUREMENTS

It has already been mentioned in sect. 2 that a measurement of the intensity of a γ-line as a function of target thickness may indicate the reaction mechanism. This method was applied in order to prove the direct reaction mechanism for residual nuclei formed from the target nucleus. For nuclei originating from the projectile the mechanism is obvious from the large Doppler effect observed (see sect. 3.1). As this work is mainly concerned with direct reactions, measurements with different target thicknesses were only carried out with 206 MeV ^{20}Ne. Some results are shown in fig. 4.

A typical case for a compound-nucleus process is ^{38}Ar. In some experiments the smaller one of the Ge detectors was placed away from 90°, and as a result the 106 keV line of ^{38}Ar showed not only a broadening but also an energy shift. The γ-rays from stopped and from recoiling nuclei were therefore easy to distinguish, even though the lifetime of the transition is only 0.26 ns. Fig. 4 shows the yield curve, which clearly indicates the large recoil. The 78 keV line of ^{32}P (τ = 0.4 ns) showed the same behavior.

A typical case for a reaction with small momentum transfer is ^{24}Na (E_γ = 472 keV, τ = 20 ms), see fig. 4. In other cases, the lifetimes are not so large, and one has to make sure that only nuclei stopped in the target are observed. The yield curve for the 417 keV line from ^{26}Al (τ = 1.8 ns) is essentially linear and the line itself shows no indication of a Doppler effect. The same arguments hold for ^{28}Al (E_γ = 31 keV, τ = 2.8 ns). We did not observe any Doppler shift of this line (upper limit 0.2%) with the small detector placed near 90° when going from the thick to the thin target, whereas the 78 keV line of ^{32}P showed a shift of 2.2% in the same spectrum. We conclude that ^{28}Al and ^{26}Al are produced from the target in neutron transfer reactions.

The lines observed from nuclei between A = 18 and 28 generally originate from states produced in reactions with small momentum transfer. This holds for the lines from ^{26}Al and ^{28}Al, for the 472 keV line from ^{24}Na, the 584 keV line from ^{22}Na (τ = 352 ns) or ^{25}Mg (4.9 ns), the 197 keV line from ^{19}F (130 ns) and the 184 keV line from ^{18}F (221 ns). The 440 keV line from ^{23}Na shows a more complex behavior. The tails on the line and the yield curve show that the first excited state of ^{23}Na or the levels decaying to it are mostly produced in compound-nucleus reactions. The direct part of the cross section is only about 30% of the total yield, as determined from the observation of a sharp component for targets thinner than the range of the compound nucleus.

3.3 EXCITATION FUNCTIONS

Excitation functions for γ-rays from nuclei produced in the reaction between ^{20}Ne and ^{27}Al are given in fig. 5. The results for nuclei with masses larger than 28 are typical for compound-nucleus reactions. The observed thresholds and maxima are in agreement with simple estimates. For instance, the reaction ^{27}Al(^{20}Ne, 3α2pn)^{32}P is expected to have a threshold at about 110 MeV beam energy, taking into consideration the Q-value and the Coulomb barrier for the evaporated particles. ^{38}Ar is produced mainly by a (^{20}Ne, 2αp) reaction, although at higher energies (^{20}Ne, α3p2n) may contribute.

The excitation functions for the nuclei in the mass region A = 18 to 28 (except ^{23}Na and ^{26}Al) show a shape similar to each other, but different from those of the heavier products mentioned above. A typical example is given by the broad component of the 351 keV line of ^{21}Ne, which is formed in a pick-up of a neutron by the ^{20}Ne projectile. The excitation function shows a threshold at about 100 MeV beam energy. This is about 50 MeV below the compound-nucleus threshold for this product. The experimental thresholds for most of the light

products, lie below those calculated for compound-nucleus reactions. The excitation function for ^{23}Na deviates somewhat from the others, which is consistent with the assumption that the compound-nucleus mechanism dominates in this case (see sect. 3.2). However, we have no explanation for the fact that the threshold for the production of the 417 keV γ-line of ^{26}Al seems to be considerably below 100 MeV.

It seems unlikely that the excitation functions given in fig. 5 merely reflect a change in the relative population of different excited states of the final nucleus. There are several arguments against this possibility: 1) The similarity of the excitation functions for all direct reactions; 2) The similarity of the excitation functions in cases where two γ-transitions were seen; 3) The fact that it is unlikely that levels with low spin should become more favored with increasing bombarding energy. Some of the transitions do start from levels of low spin.

As mentioned, some spectra on the same target have also been taken using an ^{16}O beam. The intensities of some of the γ-lines found are given in table 2. The measurements are somewhat incomplete in this case, because we did not make recoil measurements to establish the reaction mechanism. However, the excitation functions for some nuclei between A = 18 and 28, e.g. ^{26}Al and ^{28}Al, seem to be inconsistent with what is expected for compound-nucleus reactions. The spectrum taken with 165 MeV ^{16}O (fig. 2) is also strikingly similar to the one obtained with 206 MeV ^{20}Ne, particularly with respect to the relative intensities of the γ-rays from the lighter nuclei, with the exception, of course, of the broad component of the ^{21}Ne line. The data in table 2 indicate that the cross sections for direct reactions begin to increase strongly above about 120 MeV beam energy. However, the threshold seems to be less pronounced

than in the case of ^{20}Ne on ^{27}Al, probably because the cross sections below 120 MeV are already relatively high.

4. Discussion and Interpretation

It has been shown in sect. 3 that the heavier nuclei (A > 28) seen in the reaction between ^{20}Ne and ^{27}Al are produced in compound-nucleus reactions, whereas most of the lighter products (A = 18 to 28) observed originate from direct processes. The direct mechanism has been established by means of the recoil measurements discussed in sect. 3.2, which show that the momentum transfer is small compared to that in compound-nucleus reactions. In the case of ^{21}Ne, which is to a large extent formed by a pick-up of a neutron by the projectile, the reaction mechanism is obvious from the Doppler broadening of the γ-line. The fact that the thresholds observed experimentally are often considerably lower than those expected for compound-nucleus reactions followed by nucleon and α-particle emission is additional evidence for the direct-reaction mechanism. That nuclei produced by direct reactions were only observed in the mass region A = 18 to 28 and not above may, however, be due to instrumental restrictions; most of the nuclei with A = 29 to 34 do not have intense γ-transitions of low or moderate energy. Even if they do, as with ^{32}P, the possible direct part of the cross section would be hard to observe in the presence of compound-nucleus reactions.

The case of ^{23}Na indicates that a compound-nucleus mechanism may also occur for residual nuclei with A = 18 to 28, if the beam energy is above the threshold. And it is very likely that the total formation cross section for nuclei like ^{26}Al and ^{28}Al has a compound-nucleus component which we do not observe. Because of the very high angular momenta present in these heavy-ion collisions the γ-deexcitation of the residual nuclei in compound-nucleus reactions

is most likely confined to the levels with the highest spin at a given energy (the yrast levels); the transitions in ^{26}Al and ^{28}Al seen in this experiment start from states having a lower spin than the ground state, and so are bypassed in the de-excitation of the compound-nucleus. These arguments do not hold for lower beam energies, and for the case of ^{23}Na ($5/2^+ \rightarrow 3/2^+$ transition) and some other nuclei, for example ^{18}F. In the latter case, however, the direct mechanism is clear from the recoil measurement and the observed threshold.

Our measurements do not give complete information about the reaction mechanism. If they indicate a small momentum transfer for a reaction, we conclude that it cannot be a compound-nucleus reaction and therefore call it a direct reaction. But this still includes a variety of reaction mechanisms. The most important ones may be nucleon or cluster transfer, inelastic excitation, and fragmentation. The single-nucleon transfer was observed with relatively large cross sections (^{21}Ne, ^{26}Al, ^{28}Al). There are indications (^{24}Mg) that the pick-up of an α-particle might have even larger probability. The presence of elements like ^{18}F or ^{19}F made from the target nucleus ^{27}Al suggests the importance of fragmentation reactions, since a transfer of a cluster with 8 or 9 nucleons is a relatively complicated process and usually has a very low cross section. Evaporation processes following the transfer of one or two nucleons are unlikely, because low-lying levels should preferentially be populated. However, already for an α-transfer the kinematically favored Q-value[21]) is - 30 MeV, which, since the ground state Q-value is near zero, corresponds to a total excitation energy of the two residual nuclei of about that same magnitude. Thus, evaporation of nucleons after multiparticle transfer reactions might also contribute to the cross sections for ^{18}F or ^{19}F.

Up to now, we have not considered the possibility of fission of the compound-nucleus. The products of such a process are expected to have an angular distribution peaked forward and backward in the center-of-mass system. In the laboratory system, the situation will resemble very much the results for direct reactions, if one assumes a nearly symmetric fission to products with masses similar to those in the entrance channel. The backward peak will correspond to nuclei nearly at rest, the forward peak to nuclei having energies comparable to that of the projectile, thus simulating a small momentum transfer in the reaction. There are, however, several facts which makes it unlikely that compound-nucleus fission accounts for a large fraction of the cross sections observed for nuclei between A = 18 and 28. The γ-spectra obtained with different projectiles at 10 MeV/nucleon are remarkably similar with respect to the relative intensities of the lines from nuclei with A = 18 to 28, (except for the broad component of the ^{21}Ne line). This holds also for a spectrum taken with a 120 MeV ^{12}C beam. The symmetry with respect to 90° in the center-of-mass system expected for the angular distribution of fission products would require equal intensities of the broad (forward peak) and the sharp component (backward peak) of a γ-line. The actually measured ratio for the 351 keV line of ^{21}Ne is 6.6:1 in the case of the ^{20}Ne bombardment. In the ^{16}O bombardment, there does not appear to be a Doppler-broadened component at all. Further, the shape of the 440 keV line of ^{23}Na and its dependence on the target thickness is consistent with a compound-nucleus process with particle evaporation. However, because of the difficulty in observing broadened line components, it cannot be excluded entirely that some small fraction of the cross sections assigned here to reactions with small momentum transfer is due to compound-nucleus fission rather than to direct reactions.

One of the essential aims of this work was to measure the excitation functions for direct reactions in the system $^{20}Ne + {}^{27}Al$ at energies where compound-nucleus formation is increasingly hindered because of the large angular momenta between target and projectile. Most of the discussion so far was necessary in order to establish the direct mechanism in reactions leading to nuclei between A = 18 and 28. Their excitation functions, which are shown in fig. 5, do show a behavior which is opposite to the decrease of the fusion cross section at high energies[2]). There is a strong increase of the cross section for one-nucleon transfer and for more complicated direct reactions by factors of 5 to 10 or more compared to the values below a threshold observed at about 100 MeV ^{20}Ne energy. This threshold lies 60 MeV above the Coulomb barrier. It indicates the point where the angular momenta for surface collisions begin to exceed the maximum angular momentum, J_{cr}, of the compound nucleus ^{47}V. Thus, above 100 MeV, partial waves with angular momenta smaller than those for surface collisions become increasingly available for direct reactions, rather than leading to fusion.

We try to formulate this concept more quantitatively by means of a sharp-cutoff model. We use the following formulae in order to calculate the reaction cross section, σ_R, and the total compound-nucleus cross section, σ_{CN}:

$$\sigma_R = \pi \lambda\!\!\!^{-2} \sum_{L=0}^{L_{max}} (2L+1) = \pi R^2 (1-V_{CB}/E)$$

$$\sigma_{CN} = \pi \lambda\!\!\!^{-2} \sum_{L=0}^{L_c} (2L+1) = \begin{cases} \sigma_R & \text{for } L_{cr} \geq L_{max} \\ \pi \lambda\!\!\!^{-2} \cdot (L_{cr}+1)^2 \sim 1/E & \text{for } L_{cr} < L_{max} \end{cases}$$

with L_c = minimum (L_{cr}, L_{max}),

$L_{max} = k_{CB} \cdot R$, $R = r_o (A_1^{1/3} + A_2^{1/3}) + t$, $k_{CB} = \sqrt{2\mu \cdot (E-V_{CB})}\ /\hbar$. A_1, A_2

are the mass numbers of ^{20}Ne and ^{27}Al, μ the reduced mass, $\lambda\!\!\!^{-}$ the wave length, E the center-of-mass energy, and V_{CB} the Coulomb energy. The reaction cross section is calculated assuming that all collisions lead to a reaction in which the distance of closest approach becomes smaller than R. For the radius parameter, a value r_o = 1.16 fm was taken. The parameter, t, which accounts for the diffuseness and the range of nuclear forces, was determined from a fit of the measured reaction cross sections[3]) for ^{16}O on ^{27}Al to be t = 2.0 fm. The value of σ_{CN} follows from the assumption that all partial waves with an angular momentum smaller than L_{cr} ($\approx J_{cr}$) lead to compound-nucleus formation; L_{cr} is assumed to be independent of the excitation energy of the compound-nucleus. The total direct cross section has to be identified with the difference $\sigma_R - \sigma_{CN}$. We have simplified the situation in that we neglect all contributions to direct reactions at lower energies from the grazing partial waves.

The results for two values of the critical angular momentum, L_{cr}, are shown in fig. 6. The compound-nucleus cross sections reported in ref. 2 are consistent with L_{cr} = 30 $\hbar$ or a somewhat smaller value at higher bombarding energy. In this experiment, we were not able to determine the total direct cross section absolutely, however, the shape of the excitation function for direct reactions, i.e., the threshold at about 100 MeV, indicates a value L_{cr} = 35 $\hbar$ for the maximum angular momentum at which compound-nucleus reactions can occur. The difference between the two values for L_{cr} might not be significant in view of possible experimental uncertainties. The first value depends on a comparison between two separately measured absolute cross sections. The second one is mainly based on the value of the threshold energy in direct reactions, which is also not very accurate. However, if the discrepancy is real, it may be explained by the fact that fusion processes followed by fission are

not included in the cross sections of ref. 2. It is expected that compound nuclei formed with spins somewhat below L_{cr} may undergo predominantly fission.

For the compound nucleus ^{47}V, calculations[1]) using the liquid-drop model predict an upper limit $L \approx 45\ \hbar$ at which the fission barrier vanishes. However, at somewhat smaller angular momenta the barrier will still be low, and so the lifetime of this "compound-nucleus" will be short or perhaps comparable to the nuclear rotation time and of the same order as the time typical for direct reactions. The value $L = 35\ \hbar$ determined experimentally for the transition between direct and compound-nucleus reactions is therefore consistent with this picture. The theoretical estimate of the angular momentum at which the fission barrier becomes so large that particle evaporation becomes predominant is $L = 30\ \hbar$, which is in agreement with the measurements[2]).

According to the model described above, all partial waves with angular momenta between $L_{cr} = 35\ \hbar$ and L_{max}, which is about 60 $\hbar$ for 200 MeV ^{20}Ne on ^{27}Al, contribute to direct reactions. This explains the large cross sections for these processes at this energy. Assuming that the two nuclei would penetrate each other, the minimum distance between their centers can be calculated. In a collision with $L = 35\ \hbar$ at 200 MeV this distance is roughly 60% of that at which the nuclei start to interact. Therefore, one expects that strong interactions leading to multiparticle transfer and fragmentation can occur.

In this experiment, we observe only about 200 to 300 mb of the 1400 mb cross section expected for direct reactions in the system ^{20}Ne on ^{27}Al at 200 MeV. There are several reasons for this. First, we cannot observe final nuclei which are produced in the ground state. Secondly, we do not see nuclei formed from the projectile, if their lifetime for γ-de-excitation is longer than a few nanoseconds (e.g. ^{19}F and ^{19}Ne in the $5/2^+$ state). We also did not measure

γ-rays above about 600 keV, except some very intense ones. However, the largest cross sections observed for direct reactions at high energies are of the same magnitude as the largest compound-nucleus cross sections at lower energies.

5. Summary

In-beam γ-ray spectroscopy is often used for studying heavy-ion induced compound-nucleus reactions. Here, we applied this technique to direct heavy-ion reactions. The method proves to be very useful in giving a survey over a large number of reaction products. Information about the momentum transferred in a reaction and so about the reaction mechanism can be obtained. The experiments may be easily refined, e.g. by measuring γ-rays from the two residual nuclei simultaneously with a coincidence technique in order to get more detailed information about a transfer reaction.

In this work, we measured excitation functions for direct processes in heavy-ion reactions on ^{27}Al at beam energies up to 10 MeV/nucleon. The cross sections for the ^{20}Ne-induced reactions show a threshold at about 100 MeV beam energy, above which they increase strongly to values an order of magnitude larger than those below. This is a consequence of the fact that a compound nucleus can only be formed with a limited angular momentum, and so a large number of partial waves may contribute to direct processes. The latter, therefore, are no longer only surface reactions. Despite the stronger interaction expected for smaller impact parameters, the data indicate that simple transfer reactions get large cross sections. However, fragmentation processes are most likely responsible for some of the lighter products observed.

We would like to thank Drs. J. R. Leigh and K. H. Maier for their help and suggestions during the experiment, Dr. F. S. Stephens for his comments on the manuscript and especially Dr. W. J. Swiatecki for valuable discussions concerning the interpretation of the results. F. Pühlhofer acknowledges a grant from the Bundesministerium für Bildung und Wissenschaft in Bonn.

REFERENCES

1) S. Cohen, F. Plasil and W. J. Swiatecki, Proc. of the Third Conf. on Reactions Between Complex Nuclei, ed. by A. Ghiorso, R. M. Diamond and H. E. Conzett, (Univ. of California Press, Berkeley and Los Angeles, 1963), p. 325; F. Plasil and W. J. Swiatecki, Equilibrium Configurations of Rotating Charged or Gravitating Liquid Masses with Surface Tension (preprint); W. J. Swiatecki, private communication

2) L. Kowalski, J. C. Jodogne, and J. M. Miller, Phys. Rev. 169 (1968) 894

3) B. Wilkins and G. Igo, Third Conf. (see ref. 1) p. 241

4) J. B. Natowitz, Phys. Rev. C1 (1970) 623

5) T. Sikkeland and V. R. Viola, Third Conf. (see ref. 1), p. 232

6) I. M. Ladenbauer-Bellis, I. L. Preiss, and C. E. Anderson, Phys. Rev. 125 (1961) 606

7) M. A. Tamers and R. Wolfgang, Phys. Rev. 117 (1960) 812; J. B. J. Read, I. M. Ladenbauer-Bellis and R. Wolfgang, Phys. Rev. 127 (1962) 1722

8) C. E. Anderson, W. J. Knox, A. R. Quinton and G. R. Bach, Phys. Rev. Letters 3 (1959) 557

9) V. V. Volkov and J. Wilczynski, Nucl. Phys. A92 (1967) 495

10) G. F. Gridnev, V. V. Volkov and J. Wilczynski, Nucl. Phys. A142 (1970) 385

11) J. Galin, D. Guerreau, M. Lefort, J. Peter, X. Tarrago and R. Basile, Nucl. Phys. A159 (1970) 461

12) P. M. Endt and C. van der Leun, Nucl. Phys. A105 (1967) 1

13) J. A. Becker, J. W. Olness, and D. H. Wilkinson, Phys. Rev. 155 (1967) 1089

14) T. K. Alexander, K. W. Allen and D. C. Healy, Phys. Letters 20 (1966) 402

15) R. J. Nickles, Nucl. Phys. A134 (1969) 308

16) R. A. Mendelson and R. T. Carpenter, Phys. Rev. 165 (1968) 1214

17) G. A. P. Engelbertink, K. W. Jones, J. W. Olness and E. K. Warburton, Phys. Letters 33B (1970) 353

18) A. N. James, P. R. Alderson, D. C. Bailey, P. E. Carr, J. L. Durell, M. W. Greene and J. F. Sharpey-Schafer, Nucl. Phys. A172 (1971) 401

19) D. M. Gordon and R. W. Kavanagh, Phys. Rev. C4 (1971) 145

20) R. M. Diamond, A. M. Poskanzer, F. S. Stephens, W. J. Swiatecki and D. Ward, Phys. Rev. Letters 20 (1968) 802

21) P. J. Siemens, J. P. Bondorf, D. H. E. Gross, and F. Dickmann, Phys. Letters 36B (1971) 24

TABLE CAPTIONS

Table 1. Gamma rays observed in the reaction between ^{20}Ne and ^{27}Al. In column 1, the measured γ-energies are listed (±0.3 keV, except if otherwise stated). The following columns specify the nucleus and the transition. The data are from ref. 12, except if otherwise indicated. The energy of the maximum of the excitation function is only roughly estimated. Cross sections (±30%) are for the production of the γ-line, not for the total formation of a nucleus.

[a]) to [g]) = refs. 13 to 19

[h]) doublet $^{22}Na/^{25}Mg$. The cross section is split equally.

[i]) sharp component

[k]) broad component

[l]) seen in one experiment at 149 MeV with the coaxial counter

[m]) 50% branch [n]) 90% branch [o]) 22% branch

Table 2. Relative intensities of some γ-rays observed in the reaction between ^{16}O and ^{27}Al. ^{38}Ar and ^{32}P are formed in compound-nucleus reactions, the other nuclei probably in direct reactions.

Table 1

E_γ (keV)	Nucleus	Transition	τ	Maximum of Excitation Function	Cross Section	Reaction Mechanism
184.3	^{18}F	$5^+ \rightarrow 3^+$	221 ns [a]	160 MeV	7.0 mb (200 MeV)	direct
937.0	^{18}F	$3^+ \rightarrow 1^+$ g.s.	68 ps [b]		9.0 mb (200 MeV)	
109.8	^{19}F	$1/2^- \rightarrow 1/2^+$ g.s.	0.85 ns [c]	$\geq$200 MeV	3.5 mb (200 MeV)	
197.2	^{19}F	$5/2^+ \rightarrow 1/2^+$ g.s.	130 ns [a]	$\geq$200 MeV	12.0 mb (200 MeV)	direct
238.3	^{19}Ne	$5/2^+ \rightarrow 1/2^+$ g.s.	27 ns [a]	$\geq$200 MeV	2.5 mb (200 MeV)	
350.7	^{21}Ne	$5/2^+ \rightarrow 3/2^+$ g.s.	22 ps [c]	$\geq$200 MeV	{10.0 mb (200 MeV)[i] 66.0 mb (200 MeV)[k]}	direct
584[h]	^{22}Na	$1^+ \rightarrow 3^+$ g.s.	352 ns	$\geq$200 MeV	9.5 mb (200 MeV)[h]	direct
440.1	^{23}Na	$5/2^+ \rightarrow 3/2^+$ g.s.	1.6 ps	$\geq$200 MeV	56.0 mb (200 MeV)	{66% compound 33% direct}
472.4	^{24}Na	$1^+ \rightarrow 4^+$ g.s.	29 ms	$\geq$200 MeV	5.5 mb (200 MeV)	direct
90.7	^{24}Na	$(2)^+ \rightarrow 1^+$	<0.5 ns [d]	$\geq$200 MeV	1.3 mb (200 MeV)	
1368±5[l]	^{24}Mg	$2^+ \rightarrow 0^+$ g.s.	1.4 ps		150±70 mb (140 MeV)	direct
584[h]	^{25}Mg	$1/2^+ \rightarrow 5/2^+$ g.s.	4.9 ns	$\geq$200 MeV	9.5 mb (200 MeV)	direct
389.7	^{25}Mg	$3/2^+ \rightarrow 1/2^+$	7.0 ps	$\geq$200 MeV	3.0 mb (200 MeV)[m]	
416.8	^{26}Al	$3^+ \rightarrow 5^+$ g.s.	1.8 ns	$\geq$200 MeV	17.0 mb (200 MeV)	direct
30.6	^{28}Al	$2^+ \rightarrow 3^+$ g.s.	2.8 ns	$\geq$200 MeV	7.5 mb (200 MeV)	direct
1780±3[l]	^{28}Al	decay	3.3 min		23.0 mb (140 MeV)	
1780±3[l]	^{28}Si	$2^+ \rightarrow 0^+$ g.s.	0.6 ps			
78.1	^{32}P	$2^+ \rightarrow 1^+$ g.s.	0.4 ns [g]	170 MeV	24.0 mb (140 MeV)	compound
146.2	^{34}Cl	$3^+ \rightarrow 0^+$ g.s.	46.3 min	110 MeV		

Continued

Table 1 (Continued)

E_γ (keV)	Nucleus	Transition	τ	Maximum of Excitation Function	Cross Section	Reaction Mechanism
789±1	^{36}Cl	$(3)^+ \rightarrow 2^+$ g.s.		130 MeV	38.0 mb (140 MeV)	compound
105.8	^{38}Ar	$5^- \rightarrow 4^-$	260 ps [e]	70 MeV	105.0 mb (70 MeV)[n]	compound
670±1	^{38}Ar	$4^- \rightarrow 3^-$	4 ps	70 MeV	120.0 mb (70 MeV)	compound
29.9	^{40}K	$3^- \rightarrow 4^-$ g.s.	5.7 ns	$\leqslant$70 MeV	10.0 mb (70 MeV)	compound
891±1	^{40}K	$5^- \rightarrow 4^-$ g.s.	1.0 ps [f]	80 MeV	120.0 mb (70 MeV)	
1227±2	^{42}Ca	$4^+ \rightarrow 2^+$		90 MeV	40.0 mb (105 MeV)	
437.2	^{42}Ca	$6^+ \rightarrow 4^+$		90 MeV	48.0 mb (105 MeV)	compound
372.7	^{43}Ca	$5/2^+ \rightarrow 7/2^+$ g.s.		$\leqslant$70 MeV	10.8 mb (70 MeV)	compound
1156±2	^{44}Ca	$2^+ \rightarrow 0^+$ g.s.		$\leqslant$70 MeV	55.0 mb (70 MeV)	compound
1227±2	^{42m}Sc	decay	89 s		4.9 mb (70 MeV)	
437.2	^{42m}Sc	decay	89 s	80 MeV	7.0 mb (70 MeV)	compound
151.3	^{43}Sc	$3/2^+ \rightarrow 7/2^+$ g.s.	635 μs	$\leqslant$70 MeV	17.0 mb (70 MeV)[o]	compound
372.7	^{43}Sc	decay	5.7 h			
271.1	^{44}Sc	$6^+ \rightarrow 2^+$ g.s.	85 h			
1156±2	^{44}Sc	decay	5.6 h			

Table 2

E_γ (keV)	Nucleus	Relative Intensity At 88 MeV	125 MeV	160 MeV
105.8	^{38}Ar	300	14.6	4.7
78.1	^{32}P	13.5	26.5	16.0
30.6	^{28}Al	1.9	3.8	8.0
416.8	^{26}Al	8.0	11.7	27.0
472.4	^{24}Na	<1.0	2.0	7.0
197.2	^{19}F	3.8	5.6	12.8
184.3	^{18}F	2.3	4.0	8.7

FIGURE CAPTIONS

Fig. 1. Gamma-ray intensity as a function of target thickness. Case 1: γ-rays from nuclei formed from the target in a direct reaction (no momentum transfer). Case 2: γ-rays from nuclei formed in compound-nucleus reactions (full momentum transfer); this curve holds for nuclei which are stopped in the target. Gamma rays from recoiling nuclei are either absent, if the lifetime is much larger than 1 ns, or they can be distinguished by the Doppler effect. A narrow range distribution is assumed.

Fig. 2. Gamma-ray spectra obtained in the ^{20}Ne and ^{16}O bombardments of ^{27}Al.

Fig. 3. Reaction products identified in the experiment with the ^{20}Ne beam. Projectile, target and compound-nucleus are indicated by dark squares. A minus sign indicates that a nucleus has not been observed although it should be detectable in this experiment.

Fig. 4. Experimental yield functions for 206 MeV ^{20}Ne on ^{27}Al. A correction for the energy loss in the thickest target has been included. The energy of the transition and the lifetime are indicated.

Fig. 5. Excitation functions measured for ^{20}Ne on ^{27}Al. The arrows labeled CN indicate the calculated threshold for compound-nucleus reactions (with emission of nucleons and α-particles). Error bars include only statistics and errors due to background subtraction.

Fig. 6. Energy dependence of the reaction cross section, σ_R, and of the total compound-nucleus cross section, σ_{CN}, for ^{20}Ne on ^{27}Al according to the sharp-cutoff model described in the text. The curve parameter is L_{cr}, the upper limit of the angular momentum of the compound-nucleus. The data points for σ_{CN} are from ref. 2.

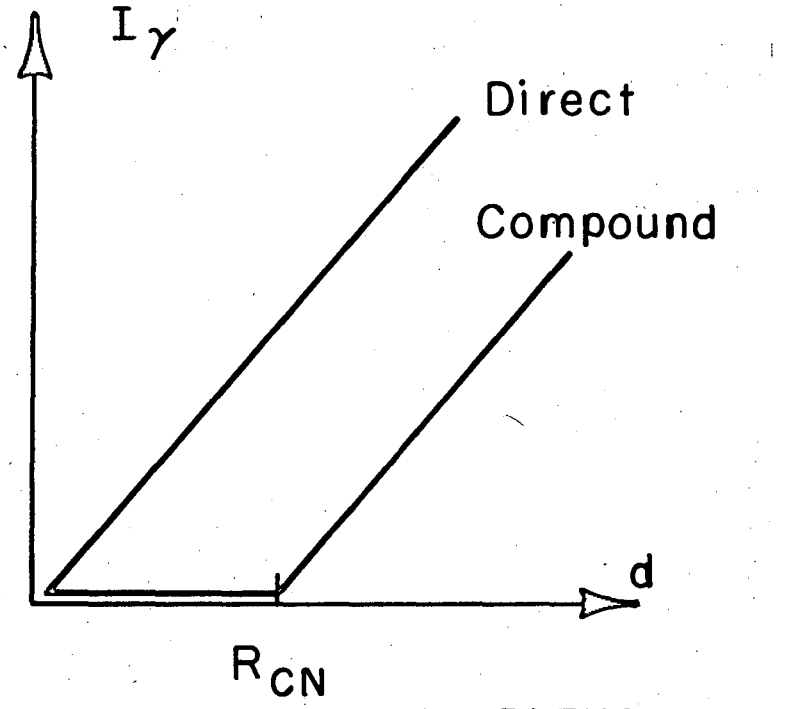

Fig. 1

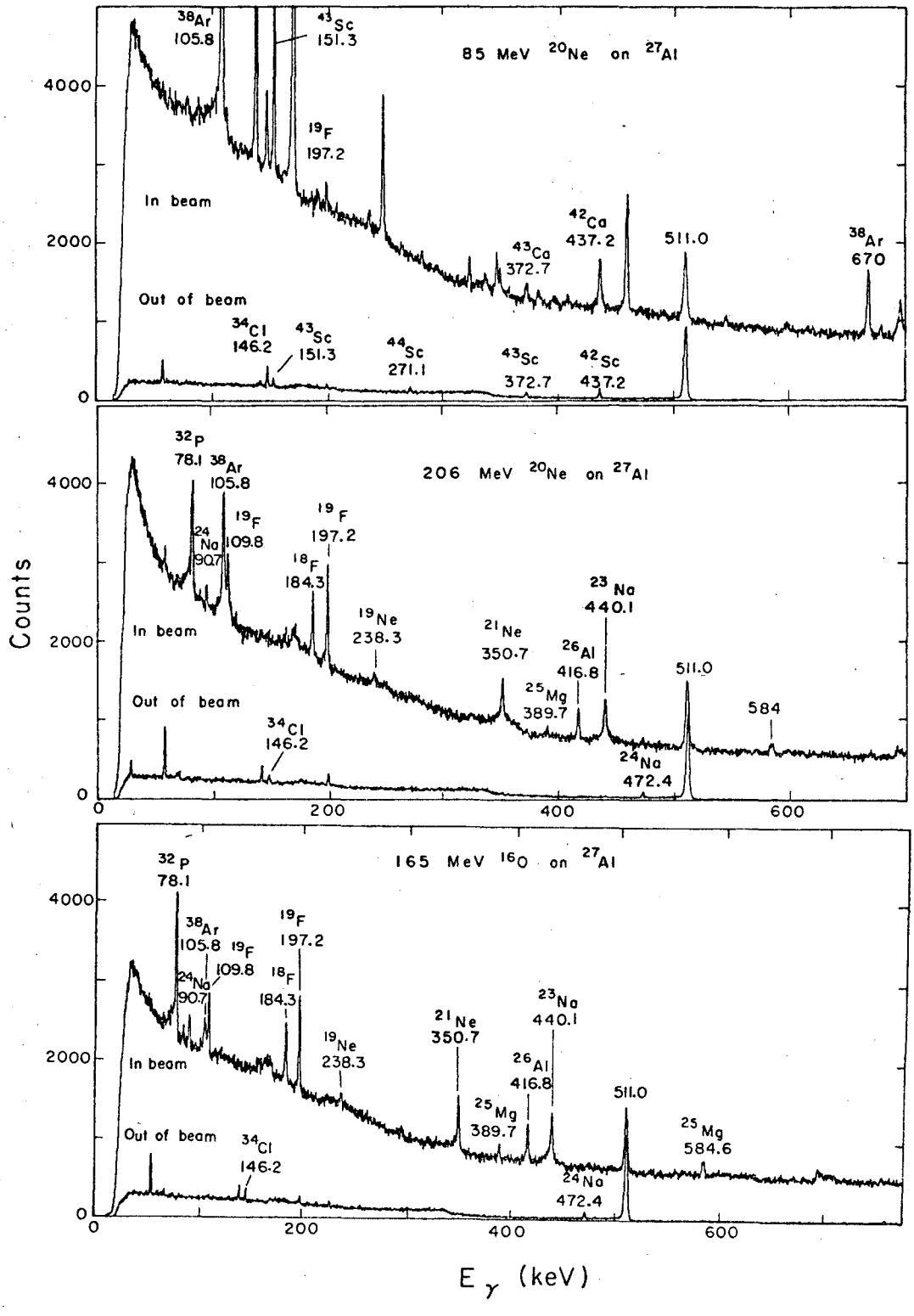
85 MeV 20Ne on 27Al
38Ar 105.8
43Sc 151.3
19F 197.2
In beam
42Ca 437.2
43Ca 372.7
511.0
38Ar 670
Out of beam
34Cl 146.2
43Sc 151.3
44Sc 271.1
43Sc 372.7
42Sc 437.2
206 MeV 20Ne on 27Al
32P 78.1
38Ar 105.8
19F 109.8
24Na 90.7
19F 197.2
18F 184.3
19Ne 238.3
21Ne 350.7
23Na 440.1
26Al 416.8
25Mg 389.7
511.0
584
24Na 472.4
165 MeV 16O on 27Al
32P 78.1
38Ar 105.8
19F 109.8
24Na 90.7
19F 197.2
18F 184.3
19Ne 238.3
21Ne 350.7
23Na 440.1
26Al 416.8
25Mg 389.7
511.0
25Mg 584.6
24Na 472.4
Counts
Eγ (keV)
XBL7115-4877

Fig. 2

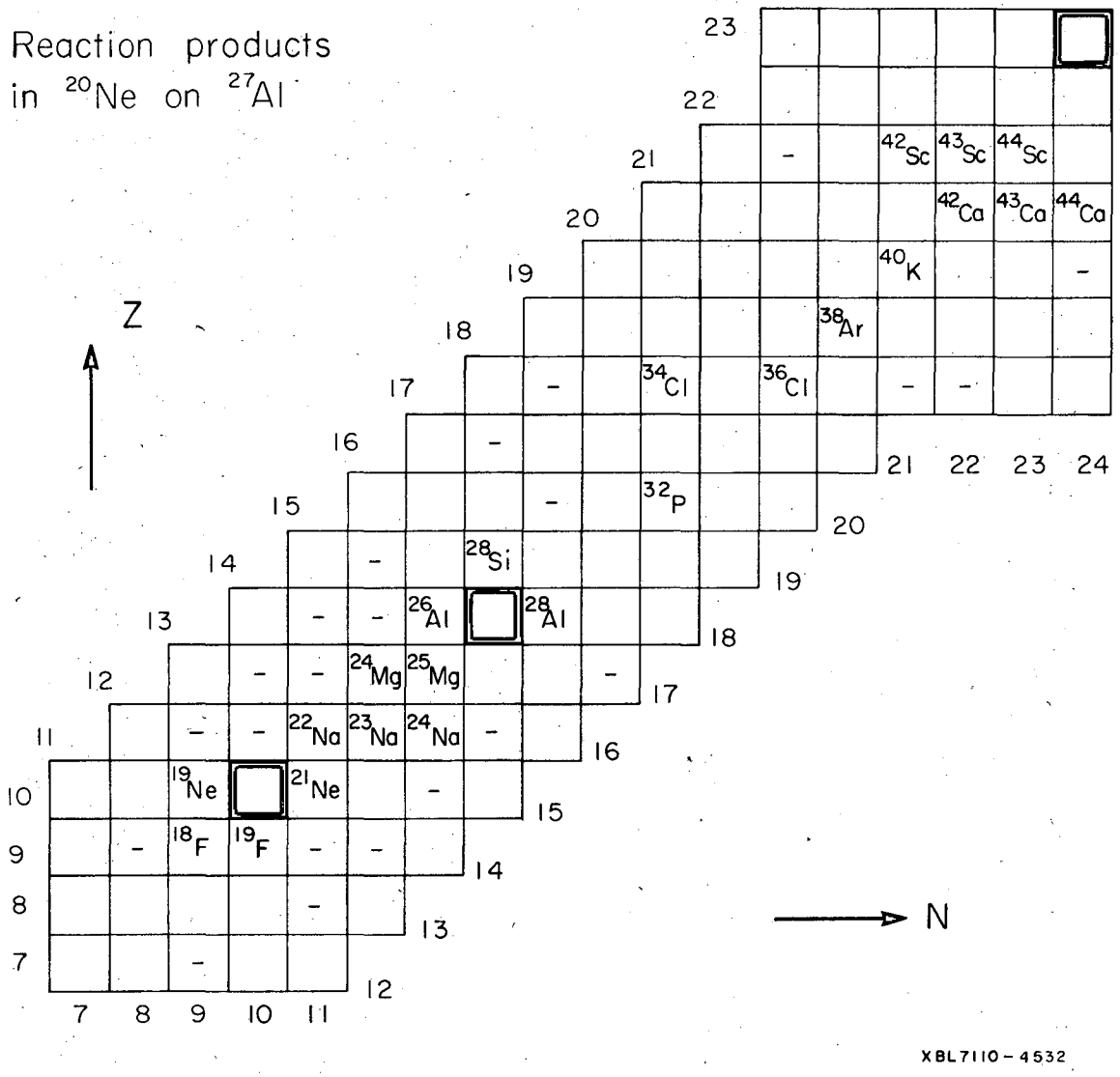
Reaction products
in ^{20}Ne on ^{27}Al
Z
N
^{19}Ne
^{21}Ne
^{18}F
^{19}F
^{22}Na
^{23}Na
^{24}Na
^{24}Mg
^{25}Mg
^{26}Al
^{28}Si
^{28}Al
^{32}P
^{34}Cl
^{36}Cl
^{38}Ar
^{40}K
^{42}Sc
^{43}Sc
^{44}Sc
^{42}Ca
^{43}Ca
^{44}Ca
XBL7110-4532

Fig. 3

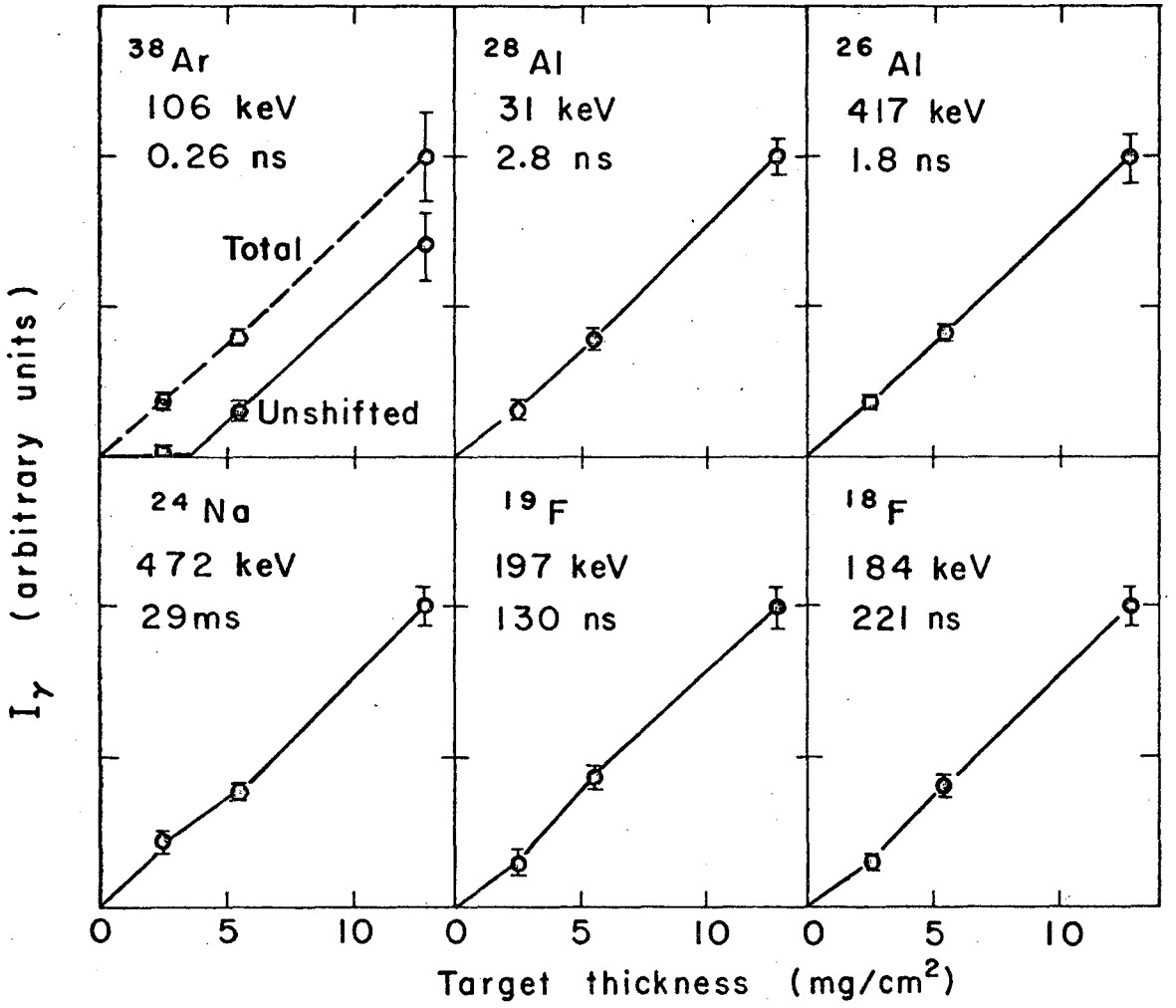

XBL7112-4875

Fig. 4

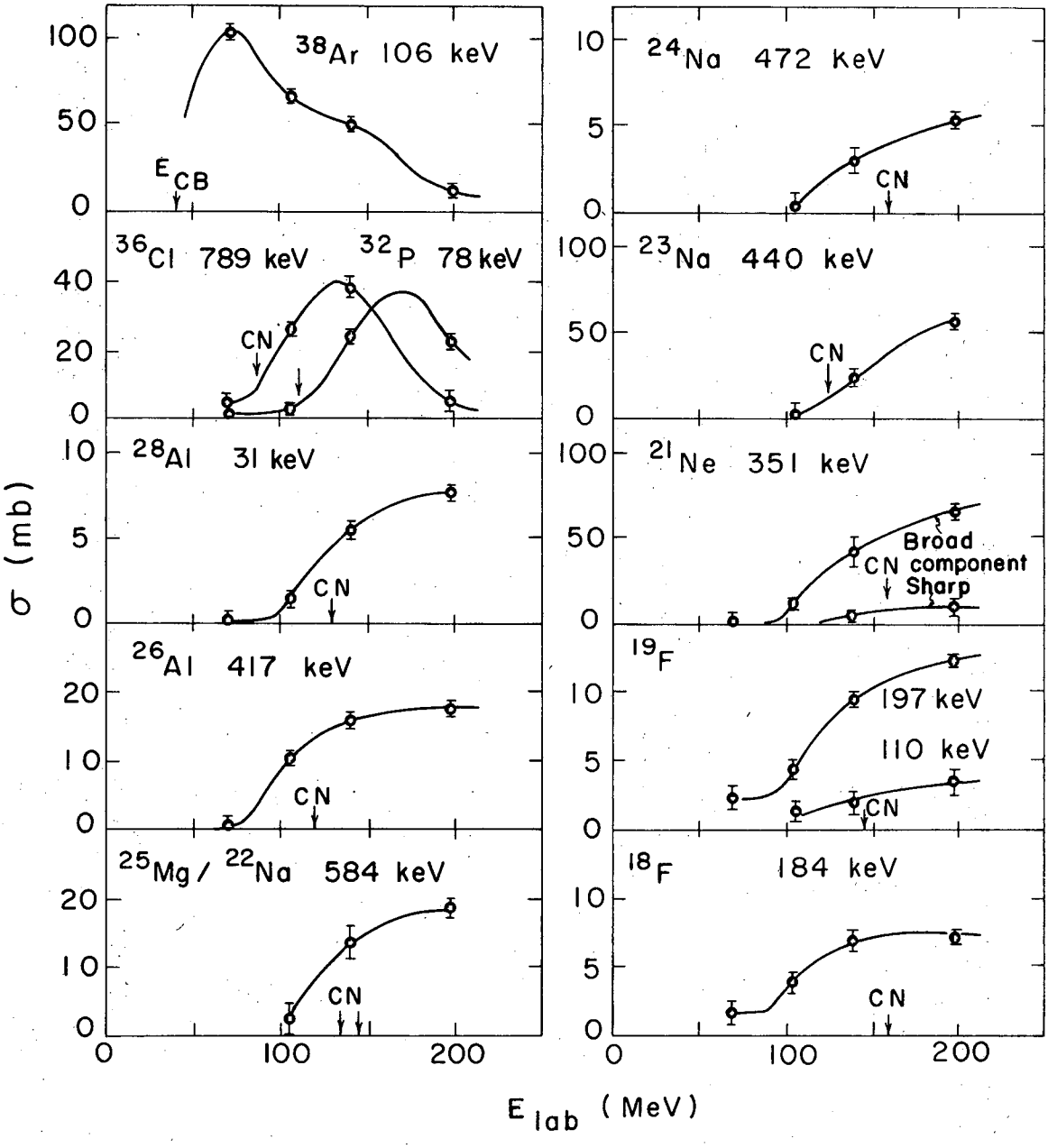
^{38}Ar 106 keV
E_{CB}
^{24}Na 472 keV
CN
^{36}Cl 789 keV
^{32}P 78 keV
CN
^{23}Na 440 keV
CN
^{28}Al 31 keV
CN
^{21}Ne 351 keV
Broad
CN component
Sharp
^{26}Al 417 keV
CN
^{19}F
197 keV
110 keV
CN
^{25}Mg / ^{22}Na 584 keV
CN
^{18}F 184 keV
CN
σ (mb)
E_{lab} (MeV)
XBL7112-4876

Fig. 5

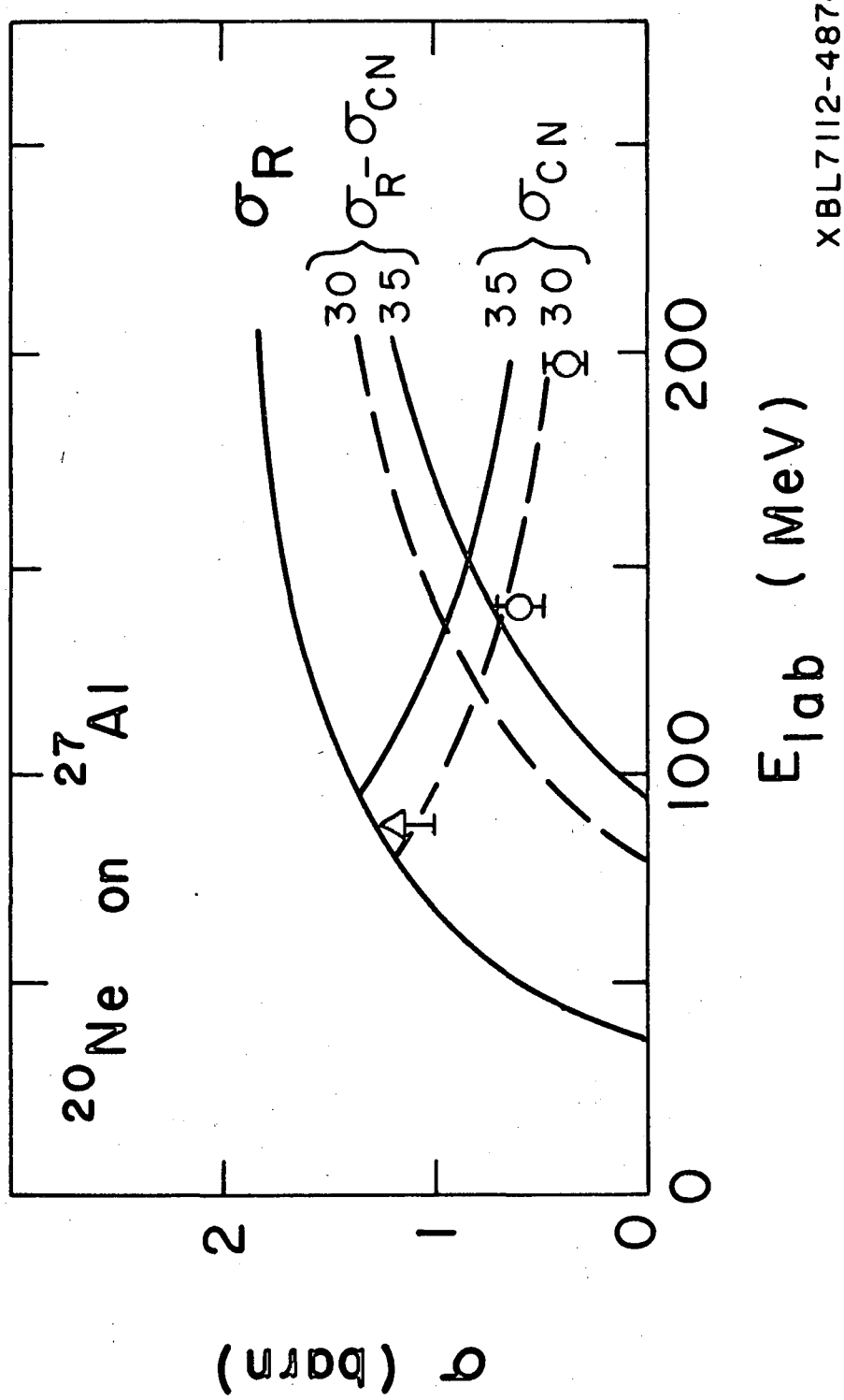
σ (barn)
2
1
0
0
100
200
E lab (MeV)
20Ne on 27Al
σR
σR-σCN
30
35
σCN
35
30
XBL7112-4874

Fig. 6

TECHNICAL INFORMATION DIVISION
LAWRENCE BERKELEY LABORATORY
UNIVERSITY OF CALIFORNIA
BERKELEY, CALIFORNIA 94720